IEEE Access
Multidisciplinary ⋮ Rapid Review ⋮ Open Access Journal

Received April 12, 2022, accepted May 24, 2022, date of publication June 1, 2022, date of current version June 6, 2022.

Digital Object Identifier 10.1109/ACCESS.2022.3179470

A Fast and Scalable Transmission Switching Algorithm for Boosting Resilience of Electric Grids Impacted by Extreme Weather Events

TANVEER HUSSAIN[1], (Graduate Student Member, IEEE), SIDDHARTH SURYANARAYANAN[1], (Senior Member, IEEE), TIMOTHY M. HANSEN[1], (Senior Member, IEEE), AND S. M. SHAFIUL ALAM[2], (Senior Member, IEEE)

[1]Electrical Engineering and Computer Science Department, South Dakota State University (SDSU), Brookings, SD 57007, USA
[2]Idaho National Laboratory (INL), Idaho Falls, ID 83402, USA

Corresponding author: Tanveer Hussain (tanveer.hussain@sdstate.edu)

This work was supported in part by INL Laboratory Directed Research and Development Program under DOE Idaho Operations Office under Contract DE-AC07-05ID14517 to Colorado State University and under Contract 5301566 and Contract 501523 to SDSU, in part by NSF under Grant 1903726, and in part by the "Roaring Thunder" Cluster at SDSU through NSF under Grant CNS-1726946.

ABSTRACT A fast and scalable heuristic transmission switching (TS) algorithm for boosting resilience by reducing the load shed in electricity networks impacted by extreme weather events (EWEs) is presented. Finding the best transmission line to switch within a suitable time is the main challenge for wider applicability of TS. Here, we propose an algorithm that: i) finds the optimal TS candidate faster than well-known algorithms; ii) is compatible with existing optimal power flow formulations; and iii) scales for larger, realistic systems. Proof-of-concept results on the IEEE 39-bus, IEEE 118-bus, and the large-scale Polish 2383-bus systems validate our claims. Further, a case study of TS for improving grid resilience in a real-life hurricane event (Harvey, 2017) using a synthetic version of Texas' ERCOT electric grid is presented for practical application. Finally, a path forward to utilize our proposed TS algorithms for evolving EWEs is discussed.

INDEX TERMS Contingency analysis, extreme weather events, high-performance computing, load shed reduction, post contingency violations, resilience, transmission switching.

I. INTRODUCTION

Resilience of electricity grids, especially when impacted by evolving extreme weather events (EWEs), has profound impacts on quality of life and the economy. Since the 1980s, the US National Oceanic and Atmospheric Administration's (NOAA) National Centers for Environmental Information (NCEI) has tracked the impact of EWEs affecting the US that caused at least $1 billion in damages. The share of tropical cyclones and severe storms in the collective damages measured using number of events, costs incurred in consumer price index (CPI)-adjusted $, and deaths caused from all EWEs in 1980–2021 is shown in Fig. 1.

A 2019 report from Oak Ridge National Laboratory (ORNL) attributed EWEs as the "leading cause of electric power outage events" with hurricanes and severe storms causing 38% of all large disruptions—i.e., affecting at least 50,000 customers–in the US electric distribution sector during 2000–2016 [2]. Reference [3] establishes the irreplaceable role of available electricity supply for return to normalcy from the aftermath of EWEs. Effective methods to maintain uninterrupted supply of electricity with minimum load shed, especially during EWEs, are imperative tools of resilience. Transmission switching (TS), a process of intentionally switching out transmission lines, reconfigures the topology of a network resulting in a new schedule of electricity flows that may favor reductions in load shed. For our purposes, we consider the reduction or recovery of load shed during an EWE as the measure of grid resilience.

The associate editor coordinating the review of this manuscript and approving it for publication was Ravindra Singh.

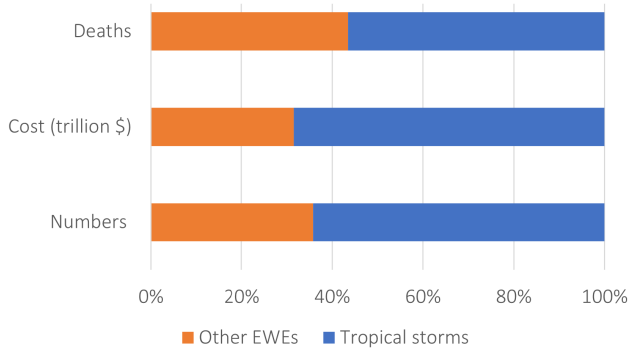

FIGURE 1. Of the 310 such EWEs from 1980–2021 that have cost a total of approximately $2.16 trillion (CPI-adjusted) and caused 15,180 deaths, the combined impact of tropical cyclones and severe storms over all the other EWEs (i.e., droughts, floods, freezes, wildfires, and winter storms) accounts for nearly 199 EWEs (64% of all EWEs), costing $1.478 trillion (CPI-adjusted, 68% of all EWEs), and causing 8577 deaths (57% of all EWEs) [1].

A. PRIOR WORK AND OUR CONTRIBUTIONS

TS may be an effective means of load shed reduction or recovery (LSR) [4]–[7], reducing line overloads [8]–[17], correcting voltage violations [13]–[15], reducing line losses [17]–[19], and for enhancing the operational resilience of power systems [20]. Researchers in [21]–[28] showed TS as an effective means for improving economic dispatch. Despite the advantages shown in existing literature, TS is not widely employed as a resiliency tool by the industry for handling LSR due to the computational complexity of the existing algorithms to find a potential TS candidate for larger systems [17], [29]. Note that we posit the use of the LSR metric as the measure of resiliency in this work—the greater the value of LSR from a TS action, the more resilient the system is upon that action.

The exhaustive search method (ESM), which sequentially runs through every potential solution for TS, is computationally expensive and intractable for realistic power system networks. A mixed integer program (MIP) based DC optimal LSR with transmission switching model (DCOLSR-TS) is presented in [4]. To reduce the computational complexity of DCOLSR-TS, a heuristic MIP (MIP-H) algorithm is presented that allows only one TS per iteration. Recently, the MIP model for AC power flows (MIPAC) was developed by modifying an existing algorithm [5]. Replacing the ESM by MIPAC for seeking the best single switching action for the IEEE 118-bus system resulted in an average speedup of approximately 2.3 times [5]. In [6], we presented the limit branches TS (LBTS) algorithm, based on line flow thresholds, which performs approximately 90 times faster than the ESM for the IEEE 118-bus system. Although LBTS is computationally fast, results showed that it is capable of recovering only 50% of load shed compared to ESM after (*N-2*) contingencies for the IEEE 118-bus system. In [7], we proposed the LSB_{max} algorithm based on selecting the candidate for TS using proximity to the load bus where the most load is expected to be shed during a contingency. The LSB_{max} algorithm performs approximately 15 times faster than the ESM for the IEEE 118-bus system and achieves an LSR of 98%. As such, the performance of the LBTS and the LSB_{max} algorithms, for the IEEE 118-bus system, indicate the need for another method for TS with faster and accurate (i.e., higher LSR) operation. Moreover, the new algorithm should be scalable to real-world larger power systems. Here we present a linear sensitivity-based TS (LiSTS) algorithm that uses line outage distribution factors (LODF), *aka* sensitivity matrix, very much like in [16] and [30] and a limit of loading on selected branches like the LBTS specifically for decreasing the load shed post contingencies.

References [4] and [5], applications of TS for LSR, are based on MIP formulations and address DC and AC optimal power flow (OPF), respectively. Proximity to contingency and violating elements based approaches for TS, intended for real-time contingency analysis and security constrained economic dispatch (SCED), were developed in [17]—however, the proximity to load shedding buses was not explored. The use of a sensitivity matrix to find the best TS candidate for reducing line overloads was presented in [8], [9], and [14]. A sensitivity matrix employing AC power flow analysis developed to improve economic dispatch (ED) was presented in [16]. A TS algorithm based on a combination of LODF and branch limits, similar to our work here, was developed in [31]; however, that work utilized only the DCOPF formulation and applied it for ED. Based on these, we note that there is still requirement of a fast and accurate TS methodology, that is indifferent to the type of OPF formulation, developed for LSR, and applied for boosting system resilience. It is in that regard we present an OPF type-agnostic TS algorithm (i.e., LiSTS) that uses LODF and a limit of loading on selected branches for resilience in electric grids.

The main contributions of this work are the development and simulation-based demonstration of a method for TS with the following features: i) no MIP based modification to OPF formulation as done in [4] and [5]; ii) combination of OPF, sensitivity matrix, and TS for LSR; iii) agnostic to the choice of DCOPF or ACOPF formulation; iv) at least one order of magnitude faster than MIPAC algorithm when seeking a single TS solution for the IEEE 118-bus system [5]; v) better LSR than the LBTS, [6]; vi) parallelizable using multiple computation cores like [17] and scalable to large-scale power systems using high-performance computing (HPC) clusters; and vii) applicable to a real-life EWE in an electric grid.

B. ASSUMPTIONS IN OUR WORK

We have considered non-trivial (*N-2*) contingencies requiring load shedding even after generation re-dispatch [4]. Similar to [6], no new OPF formulation is presented here. This manuscript focuses on a single TS candidate, and finding more than one TS candidate is out of its scope. We use MATPOWER for conducting OPF studies [32]. Dispatchable loads are modeled as ''negative generation'' with negative cost in the OPF objective function. The interested reader is

pointed to Section IV of [32] for details on the dispatchable loads and formulations of the DCOPF and ACOPF problems.

C. ORGANIZATION OF THE PAPER

This paper is organized as follows: Section II details the LiSTS algorithm. The simulation setup is described in Section III. Sections IV and V present the validation and comparative performance of the LiSTS, ESM, LBTS, and LSB_{max}. A simulation-based case study of using our proposed TS algorithms for boosting the grid's resilience during a real-life EWE is presented in section VI. Section VII concludes.

II. THE LiSTS ALGORITHM

Fig. 2 shows the flow chart of the LiSTS algorithm. First, we find the branches operating close to their limits, quantified as ρR, where $\rho \in [0, 1]$ p.u. and R is the maximum rating of a given transmission line. In our case, we have arbitrarily set $\rho = 0.99$ p.u., to identify those transmission lines henceforth called limit branches. If there exist limit branches, the sensitivity matrix [16], [30], is used to identify the top ν branches that will result in a counter flow on limit branches when subjected to TS. These ν branches are eliminated sequentially; the branch that results in the minimum load shed is the best TS candidate from the list. The main difference between the LBTS algorithm and the LiSTS algorithm is that the former removes the limit branches, whereas the latter removes the branch from the list that results in counter flow of power on limit branches. Reference [30] describes the use of sensitivity matrix and determination of counter flows. MATPOWER's inbuilt function is used to guarantee that no islands are formed after TS [33]. In our studies, we have empirically selected $\nu = 5$. The number of branches (i.e., five here) is chosen after considering the trade-off between accuracy of results and the speed of arriving at a useful solution. It is noted that the accuracy of the solution will increase and, concomitantly, the speed of the algorithm will decrease with increase in the number of branches selected.

III. SIMULATION SETUP

In this case study, we use three test systems, from MATPOWER, of increasing magnitude, namely: i) the IEEE 39-bus system [34]; ii) the IEEE 118-bus system [35], [36]; and the Polish 2383-bus system [37]. As in [4], our emergency ratings are set to 125% of normal ratings. For the first two test systems, simulations are performed on a 3.89 GHz desktop computer with 16 GB RAM and without utilizing parallel processing. This effort established a proof-of-concept of the tractability of LiSTS. For the Polish 2383-bus system, simulations are performed on compute nodes of a dedicated HPC cluster [38]. Each compute node has 40 cores and 192 GB RAM.

Table 1 shows the contingency lists (CL) for (*N-2*) non-trivial contingencies in the test systems for the DCOPF and ACOPF studies. CL-ALL includes all elements in the three types of (*N-2*) contingencies, namely, i) two generator failures (G1 & G2); ii) two non-radial line failures (L1 & L2); and iii) mixed generator and non-radial line failures (G1 & L1).

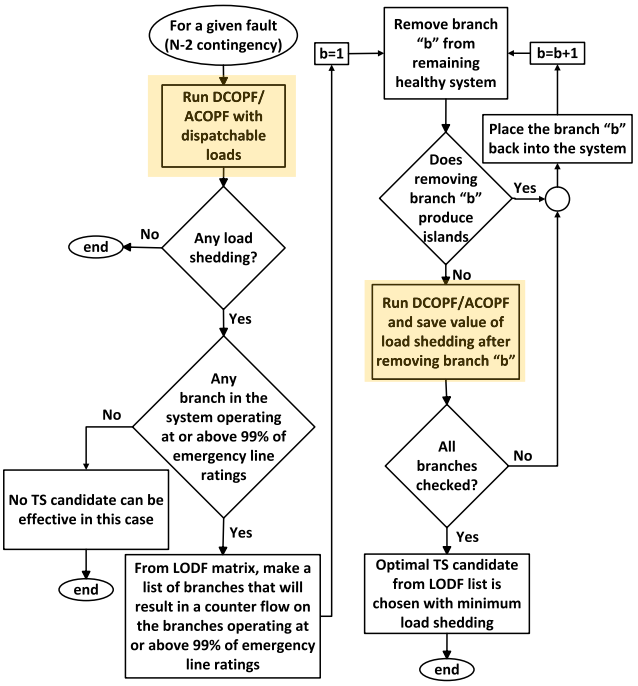

FIGURE 2. Flowchart of proposed LiSTS algorithm for finding the optimal TS candidates. The blocks shown in shaded color (orange) represent the choice of either the DCOPF or ACOPF algorithm.

TABLE 1. The number of non-trivial contingencies for the three test systems.

Test system	DCOPF/ ACOPF	CL-ALL	G1 & G2	L1 & L2	G1 & L1
IEEE 39-bus system	DCOPF	165	44	9	112
	ACOPF	90	18	4	68
IEEE 118-bus system	DCOPF	801	39	368	394
	ACOPF	3808	69	2770	969
Polish 2383-bus system	DCOPF	120	40	40	40
	ACOPF	120	40	40	40

IV. PROOF OF CONCEPT USING TEST SYSTEMS

We use two metrics, namely, percentage load shed reduction or recovery (%LSR) and relative improvement (I_{μ}^{k}), from [6], to compare the relative performance of the LiSTS with ESM. LSR in the ESM and the LiSTS algorithm are given by (1), where τ is ESM or LiSTS and (LS_i) is load shed during contingency i, $i \in \{CL\}$.

$$\text{LSR}_{\tau} = \sum_{i=1}^{CL} (LS_i)_{without\ TS} - \sum_{i=1}^{CL} (LS_i)_{\tau} \tag{1}$$

Note that ESM will result in lower or equal cumulative load shed compared to LiSTS (i.e., a higher or equal LSR value) due to the inherent nature of an exhaustive search. We use the results from ESM to normalize the LSR obtained from LiSTS, as shown in (2).

$$\%\text{LSR} = \frac{\text{LSR}_{LiSTS}}{\text{LSR}_{ESM}} \times 100 \tag{2}$$

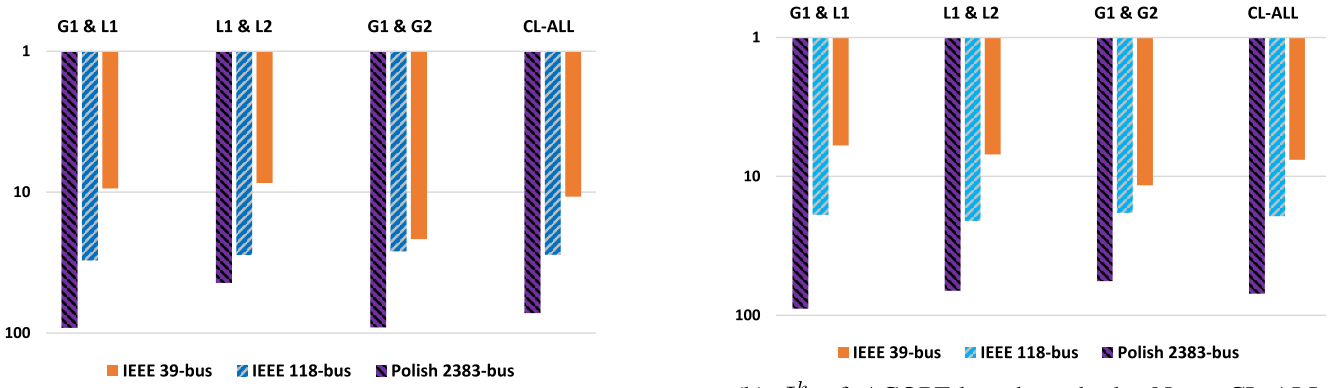

(a) I_{μ}^{k} of DCOPF-based methods

(b) I_{μ}^{k} of ACOPF-based methods. Note, CL-ALL values are from Table 3

FIGURE 3. I_{μ}^{k} **(i.e., relative computation speed) of the ESM and LiSTS algorithms, plotted on a reverse semilog for the DCOPF (3a) and ACOPF (3b) methods.**

TABLE 2. **%LSR results for the LiSTS algorithm.**

Contingency type k	DCOPF-based LiSTS			ACOPF-based LiSTS		
	IEEE 39-bus	IEEE 118-bus	Polish 2383-bus	IEEE 39-bus	IEEE 118-bus	Polish 2383-bus
CL-ALL	98.4	99.2	98.4	97.7	98	97.9
G1 & G2	100	100	100	99	99	100
L1 & L2	100	100	98	100	96	98
G1 & L1	97	99	98	96	99	95

TABLE 3. **Comparison of average computation times of *k=CL-ALL* for ACOPF-based ESM and LiSTS algorithms.**

Simulation time (s), for k = CL-ALL type contingency			
	IEEE 39-bus	IEEE 118-bus	Polish 2383-bus
ESM	2.35	28.07	46080
LiSTS	0.31	1.45	661
I_{μ}^{k}	7.58	19.36	69.71

The relative improvement (I_{μ}^{k}) is the ratio of the average computation times for contingency type k using ESM (i.e., $T_{\mu_{ESM}}^{k}$) and LiSTS (i.e., $T_{\mu_{LiSTS}}^{k}$) for finding the optimal TS candidate. Note that, i) k is either CL-ALL, (G1 & G2), (L1 & L2), or (G1 & L1), as shown in (3) and ii) the average computation time considers all the contingencies in each type k.

$$\mathrm{I}_{\mu}^{\mathrm{k}} = \frac{T_{\mu\ ESM}^{k}}{T_{\mu\ LiSTS}^{k}} \tag{3}$$

A. SIMULATION RESULTS

Table 2 shows that the %LSR achieved by the LiSTS algorithm for three test cases is approximately 95% or higher. The goal of the LiSTS algorithm is to perform computationally faster than the ESM. Fig. 3 shows the relative improvement of LiSTS with respect to the ESM. As we move from smaller to larger test systems, I_{μ}^{k} increases due to the relatively modest growth in size of the list of branches yielded by the sensitivity matrix for determining the TS candidate (see Table 3). This characteristic of scalability is useful for implementing LiSTS algorithm on real-world larger power systems. The results in Fig. 3 can be further improved by using HPC as shown in Subsection IV-B.

B. LiSTS$_P$: THE PARALLELIZED LiSTS ALGORITHM USING HPC

From Fig. 2 we observe that each iteration of the LiSTS algorithm is independent and can be executed in parallel to improve the computational efficiency. This feature is true of any sequential approach such as the ESM. We employ an HPC environment to execute the ACOPF-based LiSTS algorithm, which we name LiSTS$_p$, on the Polish 2383-bus system. The rationale for using the HPC environment only on this system is that the computational time of the LiSTS algorithm for all other test systems is already viable even without applying parallel computing. We used the built-in toolbox for parallel computing in a popular numerical modeling and simulation software, [39], for solving the ACOPF-based LiSTS algorithm on multiple compute cores. The operating system and software used are the same as those used for results shown in Fig. 3.

Fig. 4 shows the average parallel speedup, $S_{\mu_p}^{k}$, achieved for ACOPF-based LiSTS$_p$ on a reduced set of 40 contingencies in k using p cores of the HPC environment, as shown in (4). Note that the numerator and denominator of (4) represent the sequential and parallel execution times, respectively.

$$\mathrm{S}_{\mu_{\mathrm{p}}}^{\mathrm{k}} = \frac{T_{\mu\ LiSTS}^{k}}{T_{\mu\ LiSTS_p}^{k}} \tag{4}$$

Table 4 shows that $T_{\mu\ LiSTS_{p=16}}^{k}$ for ACOPF-based LiSTS$_p$ algorithm; note the $p = 16$ is chosen to represent desktop computers, and not necessarily HPCs. The inherent parallelism characteristic is useful to implement the LiSTS algorithm on real-world large power systems.

V. COMPARISONS OF LiSTS WITH LBTS AND LSB$_{MAX}$ ALGORITHMS

LBTS and LSB$_{max}$ algorithms are briefly described in Section I-A. The interested reader is pointed to [6] and [7] for details on these algorithms. Table 5 compares the

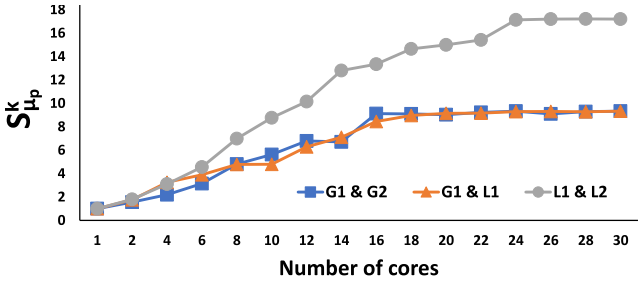

FIGURE 4. Average parallel speedup, $S^k_{\mu_p}$, versus number of cores used for running the LiSTS$_p$ algorithm on the Polish 2383-bus system.

TABLE 4. $T^k_{\mu\ LiSTS_{p=16}}$ for ACOPF-based LiSTS$_p$ algorithm. μ and σ are the mean and standard deviation, respectively.

		G1 & G2	G1 & L1	L1 & L2
$T^k_{\mu\ LiSTS_{p=16}}$ (s)	μ	62.6	61.8	66.6
	σ	7.8	13.9	10.9

TABLE 5. Comparison of the performance of LBTS, LSB$_{max}$ and LiSTS algorithms for finding the TS candidate in the IEEE 118 and Polish-2383 bus test systems. Note that the values given below are for *k=CL-ALL* for using both the DCOPF and ACOPF formulations.

		DCOPF-based algorithm		ACOPF-based algorithm	
		IEEE 118-bus	Polish 2383-bus	IEEE 118-bus	Polish 2383-bus
LBTS	%LSR	72.6	53	53.3	33
	I^k_μ	90.1	230	67.1	190.3
LSB$_{max}$	%LSR	98	100	87	100
	I^k_μ	15.4	64.3	13.5	65.1
LiSTS	%LSR	99.2	98.4	98	97.9
	I^k_μ	27.8	72.3	19.4	69.7

performance of the LiSTS algorithm with those of the LBTS and the LSB$_{max}$ algorithms. Note that the %LSR and I^k_μ for each algorithm are calculated with respect to the innate ESM, i.e., using (2) and (3), respectively. By transitivity, we can establish the comparison of the LiSTS, LSB$_{max}$, and LBTS algorithms through their respective ESM. The LiSTS is slower, but achieves a higher %LSR than LBTS. The LiSTS is faster than LSB$_{max}$ and achieves similar %LSR as LSB$_{max}$.

VI. AN APPLICATION OF TS ALGORITHMS TO A REAL-LIFE *EWE* AFTERMATH

A. HURRICANE HARVEY

Hurricane Harvey was an EWE that made landfall in Rockport, TX, on August 25, 2017, at 22:00 Central Daylight Time with an intensity of Category 4 on the Saffir-Simpson hurricane scale. Costing an estimated $133 billion (CPI adjusted, 2021) and directly resulting in 68 deaths [40], this event also left 1.67 million electricity customers without power in ERCOT's footprint.[1] These outages and the cooler temperatures accompanying Hurricane Harvey depressed the load in ERCOT in the range of 15–20 GW from that expected on a typical August afternoon. Fig. 5 depicts the loads in the eight areas of ERCOT at 22:00 on August 25, 2017–when Hurricane Harvey made landfall–and on August 18, 2017–a week prior to the event. This plot also shows the relative difference, in %, of the loads in the Coast (28%), South (30%), and South

[1]Electric Reliability Council of Texas (ERCOT) is the grid operator for nearly 90% of Texas' electric power load.

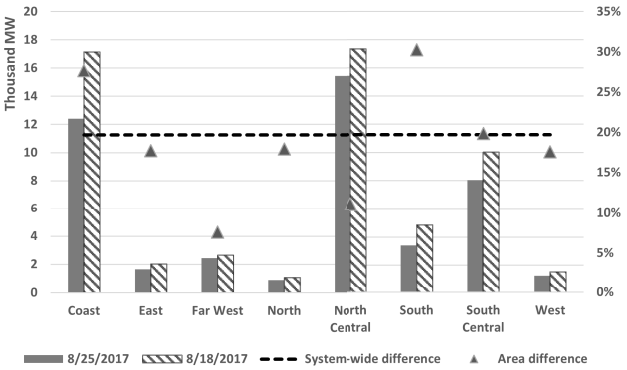

FIGURE 5. ERCOT area loads at 22:00 on 8/18/2017 (hatched bars) and 8/25/2017 (solid bars). Primary y-axis (left) shows these loads in 1000s of MW. Secondary y-axis (right) shows the percentage scale for the relative difference in area loads, which are marked by triangles. A dashed line shows the system-wide relative difference for the loads at 22:00 on the two days.

Central (20%) areas of ERCOT were at least equal to the system-wide relative difference of 20% [41] between those two dates. This higher percentage difference can be directly attributed to disruptions from Hurricane Harvey based on its inland path in Texas shown by the green line in Fig. 6. Harvey entered Texas as a Category 4 hurricane at Rockport and traveled in a northwesterly direction, progressively losing intensity and becoming a Category 1 storm near Goliad, after which it moved out of Texas in a southeasterly direction–the directions are indicated with arrowheads in Fig. 6.

Over 90 substations, 850 transmission structures, and nearly seven times as many distribution poles were damaged (or downed) due to Hurricane Harvey leading to the replacement of approximately 800 miles of electricity lines in ERCOT [42]. Fig. 7 shows the numerical proportion of the 438 transmission facilities or assets in ERCOT that were affected by Hurricane Harvey.

B. SIMULATION SETUP

Simulations for this case study are performed on a 2.10 GHz desktop computer with 32 GB RAM and without utilizing parallel processing. We used a different desktop for this case study for the following reason: in the earlier comparative study involving smaller test systems, we were not constrained by the availability of a dedicated license (PowerWorld [43] full version); for the latter case study involving the ERCOT system with 1000s of buses, we had to resort to using the full version of the software, which was only installed in our lab on the said 2.10 GHz desktop computer with 32 GB RAM. However, we have noted that the two case studies are not dependent on one another. All the algorithms in each case study should be, and are, simulated on the same desktop for comparison.

We used a high quality model of a synthetic version of the ERCOT electric grid developed by researchers from Texas A&M University using public domain information under an ARPA-E project [44]. It is pertinent to note that this model

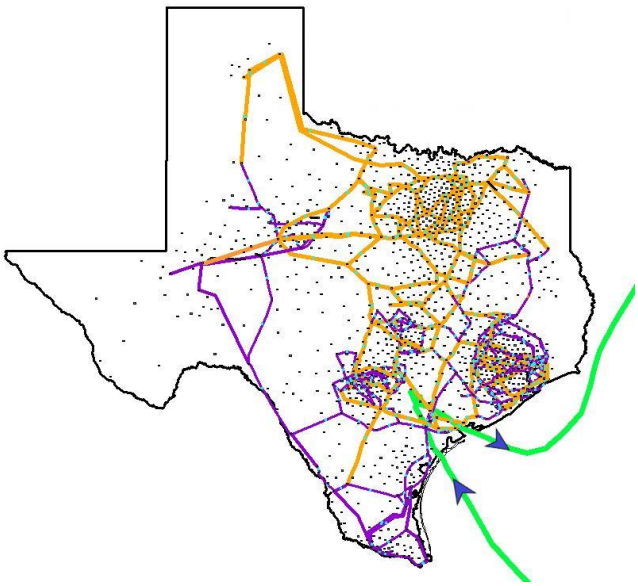

FIGURE 6. Path of Hurricane Harvey through southern texas after making landfall at 22:00 on 8/25/2017. The directions of arrival and departure of this EWE are indicated using solid blue arrowheads.

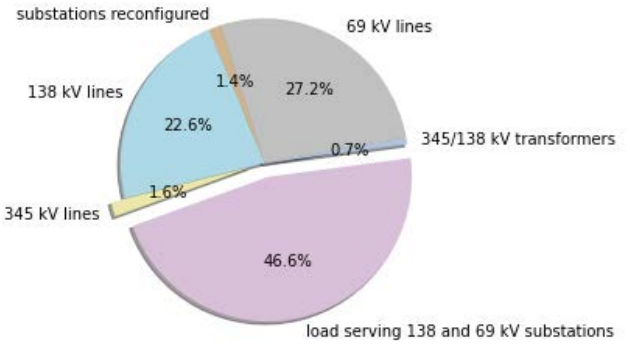

FIGURE 7. 438 transmission facilities or assets in ERCOT affected by Hurricane Harvey. Figure created using data from [42].

does not contain any critical electric infrastructure information. This model, created in the footprint of ERCOT, includes geographical similarity and associated geographical information systems (GIS) information, 2000 buses, 544 generators, 3206 lines at 500/230/161/115 kV, and area information. A GIS shape file of the path of Hurricane Harvey, obtained from [45], is superimposed on this grid model–this is shown in Fig. 6. We modeled the outage of 11 high voltage lines from Rockport to Goliad to account for the damage to the transmission grid as Harvey lost intensity from Category 4 to 1. The details of the affected transmission lines are shown in Table 6. The generation type affected mostly by these actions is natural gas (NG) units. Reference [42] reports 3043 MW and 5679 MW of shut-downs or scaled operation of generators in ERCOT prior to and after Hurricane Harvey's landfall, respectively.

Our simulation takes into account the generation that was shut-down or derated, either in anticipation or as an aftermath of the hurricane, as shown in Fig. 8. Observe that our model

TABLE 6. Transmission lines in the synthetic ERCOT grid affected by Hurricane Harvey from the simulation scenario.

From bus		To bus		Nominal voltage
Name	Number	Name	Number	(kV)
Refugio 0	4149	Rockport 0	4018	115
Victoria 3 1	7275	Fannin 1	4029	115
Premont 0	4029	Yorktown 0	6253	230
Goliad 0	4178	Yorktown 0	6253	230
YorkTown 0	6253	Nordheim 0	6329	230
Victoria 3 0	7274	Port Lavaca	7029	230
Fannin 0	4028	Victoria 3 0	7274	230
Fannin 0	4028	Victoria 3 0	7274	230
Yoakum 0	6263	Victoria 3 0	7274	230
Nursery 1	6030	Victoria 3 0	7274	230
Elmendorf 0	6239	Victoria 1 0	7414	500

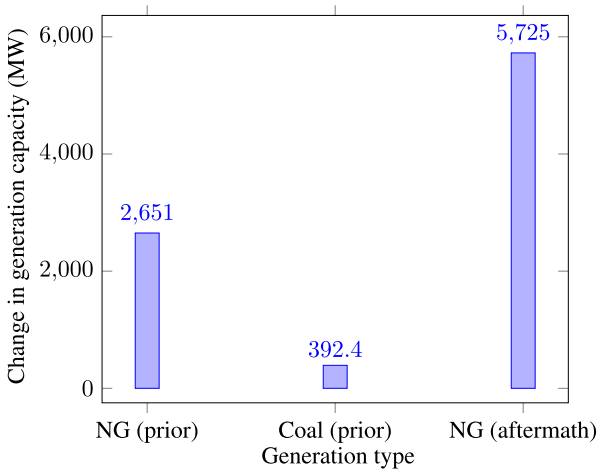

FIGURE 8. 8769 MW of generation shut-down or derated in the synthetic ERCOT grid prior to or in the aftermath of Hurricane Harvey's landfall. Data corresponding to this figure is given in Table 7.

depicts this faithfully within 6% of the actual generation turned off. Detailed load information, which is represented in aggregate in Fig. 5, and the 11 contingencies mentioned above are modeled. Upon running the simulation, we observe from Fig. 9 that 147.7 MW of load is shed. Of this amount, 5.8% (8.7 MW) belongs to a portion of the system that is isolated from the transmission grid–thus, TS actions will not be effective to reduce this component. When ESM-based TS is run as a base case, 30% (45 MW) of the load shed is identified as the potential target (or upper bound) for the achievable LSR. This leaves nearly 64% (94 MW) of the load shed unrecoverable.

C. RESULTS

The results of applying the three TS algorithms (i.e., LBTS, LSB_{max}, and LiSTS), and comparing their performances with the ESM for finding the best TS candidate for the Hurricane Harvey scenario in the synthetic ERCOT grid is shown in Table 8.

We observe that the ESM method has discovered the best TS candidate (i.e., line number 12), which recovers 45 MW of the 194 MW of load shed; however, the time to arrive at this solution is nearly 2.5 hours. As expected, LBTS is the fastest to arrive at a solution (within 1 minute); however,

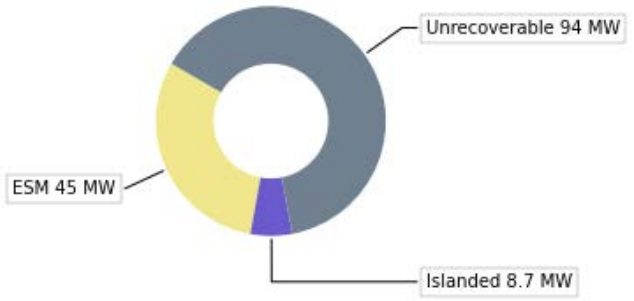

FIGURE 9. Numerical proportions of load shed in the simulated system modeling Hurricane Harvey.

TABLE 7. Generation shut-down or derated in the synthetic ERCOT grid prior to or in the aftermath of Hurricane Harvey's landfall.

Time of action	Action	Area	Generation type	Bus number	Change in capacity (MW)
Prior to storm	Taken offline	South	Natural gas	4052	2651
				4058–4063	
				4065	
				4075–4077	
				4082–4085	
	Derated		Coal	4030	392
Total generation capacity affected prior to storm					3044
Aftermath	Taken offline	South	Natural gas	7414	102
				7406	373
				7307–7311	485
				7061–7066	690
				7045–7046	377
				7021–7024	212
				6164–6167	940
				6145–6149	2546
Total generation capacity affected after the storm					5725
Total generation capacity affected due to the storm					8769

this TS solution (i.e., line number 30) recovers only 15% of the potential target LSR of 45 MW, thus rendering it unsatisfactory. Both the LSB_{max} and the LiSTS algorithms successfully discover the same TS candidate as the ESM, but the time taken to arrive at this solution is 1.5 and 3.2 minutes, respectively. We postulate following to explain the faster computational time of the LSB_{max} algorithm compared to the LiSTS algorithm. In this simulation scenario of Hurricane Harvey's impact on the synthetic ERCOT grid, we considered 11 contingencies in the system (see Table 6). The resulting rerouting of power may stress the system by (nearly) overloading the extant transmission lines. The computation time of the LiSTS algorithm is dependent on the number of branches operating at or near the rating (termed limit branches) in the system, and increases proportionally with system stress. On the other hand, the LSB_{max} algorithm, independent of this type of system stress, uses the bus where the maximum load shedding is expected to occur as the starting point for discovering the solution. Thus, the computation time of the LSB_{max} algorithm is smaller than the LiSTS for the Hurricane Harvey case study.

At the time of writing this manuscript, ERCOT has filed a petition with the Public Utility Commission of Texas to increase the value of lost load (VoLL) to \$20,000 [46]. VoLL is an estimate of the value of 1 MWh of electric energy that is not supplied. Using this proposed VoLL, the time of restoration identified in [42] as 13 days (not counting the day of landfall), and the 45 MW LSR from the simulation scenario, we can conjecture that nearly \$281 million may have been deferred from the \$133 billion of the estimated economic impact of Hurricane Harvey.

TABLE 8. Comparison of performance of methods of TS for LSR applied to the Hurricane Harvey simulation scenario.

Method	Best TS candidate	LSR after TS (MW)	Total time to solution (s)
ESM	12	45	8985
LBTS	30	6.5	51
LSB_{max}	12	45	91
LiSTS	12	45	191

D. A PATH FORWARD

NOAA's National Hurricane Center (NHC) and collaborators developed and deployed a high-resolution computer model, called hurricane weather research and forecasting (HWRF) for tracking hurricane paths and intensity in 2007. This model is run on-demand with inputs from various sources for tracking active tropical storms. HWRF is run every six hours (00:00, 6:00, 12:00, and 18:00) in a 24-hour period, with each run producing a forecast for every three hours from the start of the event to 126 hours [47]. With the availability of updated results from these models every six hours, we can predict the path and intensity of the oncoming tropical storm and run the simulations for identifying the TS candidate proactively, even for larger real life systems. With the information to switch out transmission lines ready, the system operator may have better situational awareness to decrease any load shed following the impact of the EWE, thus boosting the resilience of the electricity grid during said EWE.

VII. CONCLUSION

Here we modified an existing TS algorithm and developed the LiSTS algorithm for boosting grid resilience, which we compute as the reduction in load shed after (*N*-2) non-trivial contingencies. LiSTS performs faster than ESM by decreasing the number of branches checked for finding the optimal TS candidate. Like ESM, LiSTS is compatible with DCOPF and ACOPF-based methods. Simulation results from three standard test systems show the computational superiority of LiSTS over ESM. Parallelization of the ACOPF-based LiSTS algorithm on an HPC environment significantly improved computational efficiency for the large-scale test system. Further, we applied these TS algorithms to a simulation-based scenario of the Hurricane Harvey's impact on a synthetic version of Texas grid and demonstrated the usefulness of the LiSTS algorithm as a resilience tool.

DISCLAIMER

Parts of this work were conducted at Colorado State Univ. (CSU) and appears in a patent filed by CSU [48].

REFERENCES

[1] NOAA National Centers for Environmental Information (NCEI). (2022). *U.S. Billion-Dollar Weather and Climate Disasters*. Accessed: Jan. 28, 2022. [Online]. Available: https://www.ncdc.noaa.gov/billions/

[2] M. R. Allen-Dumas, K. C. Binita, and C. I. Cunliff, "Extreme weather and climate vulnerabilities of the electric grid: A summary of environmental sensitivity quantification methods," Oak Ridge Nat. Lab., Oak Ridge, TN, USA, Tech. Rep. ORNL/TM-2019/1252, 2019. Accessed: Jan. 28, 2022. [Online]. Available: https://bit.ly/3g7KY8Q

[3] C. Abbey, D. Cornforth, N. Hatziargyriou, K. Hirose, A. Kwasinski, E. Kyriakides, G. Platt, L. Reyes, and S. Suryanarayanan, "Powering through the storm: Microgrids operation for more efficient disaster recovery," *IEEE Power Energy Mag.*, vol. 12, no. 3, pp. 67–76, May 2014.

[4] A. R. Escobedo, E. Moreno-Centeno, and K. W. Hedman, "Topology control for load shed recovery," *IEEE Trans. Power Syst.*, vol. 29, no. 2, pp. 908–916, Mar. 2014.

[5] W. E. Brown and E. Moreno-Centeno, "Transmission-line switching for load shed prevention via an accelerated linear programming approximation of AC power flows," *IEEE Trans. Power Syst.*, vol. 35, no. 4, pp. 2575–2585, Jul. 2020.

[6] T. Hussain, S. Suryanarayanan, T. M. Hansen, and S. M. S. Alam, "A computationally improved heuristic algorithm for transmission switching using line flow thresholds for load shed reduction," in *Proc. IEEE Madrid PowerTech*, Jun. 2021, pp. 1–6.

[7] T. Hussain, S. M. S. Alam, T. M. Hansen, and S. Suryanarayanan, "The LSB_{max} algorithm for boosting resilience of electric grids post (N-2) contingencies," *J. Eng.*, vol. 2021, no. 12, pp. 807–816, Dec. 2021, doi: 10.1049/tje2.12081.

[8] A. A. Mazi, B. F. Wollenberg, and M. H. Hesse, "Corrective control of power system flows by line and bus-bar switching," *IEEE Power Eng. Rev.*, vol. PER-6, no. 8, pp. 258–264, Aug. 1986.

[9] R. Bacher and H. Glavitsch, "Network topology optimization with security constraints," *IEEE Power Eng. Rev.*, vol. PER-6, no. 11, pp. 34–35, Nov. 1986.

[10] A. G. Bakirtzis and A. P. S. Meliopoulos, "Incorporation of switching operations in power system corrective control computations," *IEEE Trans. Power Syst.*, vol. PWRS-2, no. 3, pp. 669–675, Aug. 1987.

[11] G. Schnyder and H. Glavitsch, "Integrated security control using an optimal power flow and switching concepts," *IEEE Trans. Power Syst.*, vol. PWRS-3, no. 2, pp. 782–790, May 1988.

[12] J. N. Wrubel, P. S. Rapcienski, K. L. Lee, B. S. Gisin, and G. W. Woodzell, "Practical experience with corrective switching algorithm for on-line applications," *IEEE Trans. Power Syst.*, vol. 11, no. 1, pp. 415–421, Feb. 1996.

[13] W. Shao and V. Vittal, "Corrective switching algorithm for relieving overloads and voltage violations," *IEEE Trans. Power Syst.*, vol. 20, no. 4, pp. 1877–1885, Nov. 2005.

[14] W. Shao and V. Vittal, "BIP-based OPF for line and bus-bar switching to relieve overloads and voltage violations," in *Proc. IEEE PES Power Syst. Conf. Expo.*, Oct. 2006, pp. 2090–2095.

[15] M. Khanabadi, H. Ghasemi, and M. Doostizadeh, "Optimal transmission switching considering voltage security and N-1 contingency analysis," *IEEE Trans. Power Syst.*, vol. 28, no. 1, pp. 542–550, Feb. 2013.

[16] J. D. Lyon, S. Maslennikov, M. Sahraei-Ardakani, T. Zheng, E. Litvinov, X. Li, P. Balasubramanian, and K. W. Hedman, "Harnessing flexible transmission: Corrective transmission switching for ISO-NE," *IEEE Power Energy Technol. Syst. J.*, vol. 3, no. 3, pp. 109–118, Sep. 2016.

[17] X. Li, P. Balasubramanian, M. Sahraei-Ardakani, M. Abdi-Khorsand, K. W. Hedman, and R. Podmore, "Real-time contingency analysis with corrective transmission switching," *IEEE Trans. Power Syst.*, vol. 32, no. 4, pp. 2604–2617, Jul. 2017.

[18] R. Bacher and H. Glavitsch, "Loss reduction by network switching," *IEEE Trans. Power Syst.*, vol. PWRS-3, no. 2, pp. 447–454, May 1988.

[19] S. Fliscounakis, F. Zaoui, G. Simeant, and R. Gonzalez, "Topology influence on loss reduction as a mixed integer linear programming problem," in *Proc. IEEE Lausanne Power Tech*, Jul. 2007, pp. 1987–1990.

[20] M. Mahzarnia, M. P. Moghaddam, P. T. Baboli, and P. Siano, "A review of the measures to enhance power systems resilience," *IEEE Syst. J.*, vol. 14, no. 3, pp. 4059–4070, Sep. 2020.

[21] X. Liu, Y. Wen, and Z. Li, "Multiple solutions of transmission line switching in power systems," *IEEE Trans. Power Syst.*, vol. 33, no. 1, pp. 1118–1120, Jan. 2018.

[22] Y. Sang and M. Sahraei-Ardakani, "The interdependence between transmission switching and variable-impedance series FACTS devices," *IEEE Trans. Power Syst.*, vol. 33, no. 3, pp. 2792–2803, May 2018.

[23] S. Fattahi, J. Lavaei, and A. Atamturk, "A bound strengthening method for optimal transmission switching in power systems," *IEEE Trans. Power Syst.*, vol. 34, no. 1, pp. 280–291, Jan. 2019.

[24] X. Li and K. W. Hedman, "Enhanced energy management system with corrective transmission switching strategy—Part I: Methodology," *IEEE Trans. Power Syst.*, vol. 34, no. 6, pp. 4490–4502, Nov. 2019.

[25] X. Li and K. W. Hedman, "Enhanced energy management system with corrective transmission switching strategy—Part II: Results and discussion," *IEEE Trans. Power Syst.*, vol. 34, no. 6, pp. 4503–4513, Nov. 2019.

[26] M. Sheikh, J. Aghaei, A. Letafat, M. Rajabdorri, T. Niknam, M. Shafie-Khah, and J. P. Catalão, "Security-constrained unit commitment problem with transmission switching reliability and dynamic thermal line rating," *IEEE Syst. J.*, vol. 13, no. 4, pp. 3933–3943, Dec. 2019.

[27] J. Belanger, L. A. Dessaint, and I. Kamwa, "An extended optimal transmission switching algorithm adapted for large networks and hydro-electric context," *IEEE Access*, vol. 8, pp. 87762–87774, 2020.

[28] Z. Yang and S. Oren, "Line selection and algorithm selection for transmission switching by machine learning methods," in *Proc. IEEE Milan PowerTech*, Jun. 2019, pp. 1–6.

[29] M. Sahraei-Ardakani, X. Li, P. Balasubramanian, K. W. Hedman, and M. Abdi-Khorsand, "Real-time contingency analysis with transmission switching on real power system data," *IEEE Trans. Power Syst.*, vol. 31, no. 3, pp. 2501–2502, May 2016.

[30] A. A. Mazi, B. F. Wollenberg, and M. H. Hesse, "Corrective control of power system flows by line and bus-bar switching," *IEEE Trans. Power Syst.*, vol. PWRS-1, no. 3, pp. 258–264, Aug. 1986.

[31] C. Liu, J. Wang, and J. Ostrowski, "Heuristic prescreening switchable branches in optimal transmission switching," *IEEE Trans. Power Syst.*, vol. 27, no. 4, pp. 2289–2290, Nov. 2012.

[32] R. D. Zimmerman, C. E. Murillo-Sánchez, and R. J. Thomas, "MATPOWER: Steady-state operations, planning, and analysis tools for power systems research and education," *IEEE Trans. Power Syst.*, vol. 26, no. 1, pp. 12–19, Feb. 2011.

[33] Matpower. *Find_Islands*. Accessed: Sep. 5, 2021. [Online]. Available: https://tinyurl.com/yvb5jkfs

[34] Matpower. *Case39*. Accessed: Sep. 5, 2021. [Online]. Available: https://tinyurl.com/925xstf3

[35] S. Blumsack, *Network Topologies and Transmission Investment Under Electric-Industry Restructuring*. Pittsburgh, PA, USA: Carnegie Mellon Univ., 2006.

[36] Matpower. *Case118*. Accessed: Sep. 5, 2021. [Online]. Available: https://tinyurl.com/sr93fc7a

[37] Matpower. *Case2383wp*. Accessed: Sep. 5, 2021. [Online]. Available: https://tinyurl.com/bc3mefnx

[38] South Dakota State University. *Research Computing*. Accessed: Oct. 5, 2020. [Online]. Available: https://tinyurl.com/y5xto7ng

[39] MathWorks. *Parallel Computing Toolbox*. Accessed: Sep. 5, 2021. [Online]. Available: https://tinyurl.com/yyrqj9uo

[40] E. S. Blake and D. A. Zelinsky. (May 2018). *Tropical Cylcone Report: Hurricane Harvey*. Accessed: Jan. 28, 2022. [Online]. Available: https://bit.ly/3quUwRN

[41] ERCOT. *Hourly Load Data Archives*. Accessed: Jan. 29, 2022. [Online]. Available: https://bit.ly/3oc0ll3

[42] NERC. (Mar. 2018). *Hurricane Harvey Event Analysis Report*. Accessed: Jan. 28, 2022. [Online]. Available: https://bit.ly/3HgRG8q

[43] PowerWorld Corporation. *PowerWorld Simulator*. Accessed: Sep. 5, 2021. [Online]. Available: https://www.powerworld.com/

[44] A. B. Birchfield, T. Xu, K. M. Gegner, K. S. Shetye, and T. J. Overbye, "Grid structural characteristics as validation criteria for synthetic networks," *IEEE Trans. Power Syst.*, vol. 32, no. 4, pp. 3258–3265, Jul. 2017.

[45] National Hurricane Center, NOAA. *NHC GIS Archive–Tropical Cyclone Best Track*. Accessed: Jan. 29, 2022. [Online]. Available: https://tinyurl.com/dpkdwy2t

[46] Potomac Economics. (Oct. 2021). *Executive Summary of Potomac Economics Market Redesign Proposals*. Accessed: Jan. 30, 2022. [Online]. Available: https://bit.ly/3lvmERjN

[47] National Weather Service. *HWRF Model Forecast Documentation*. Accessed: Jan. 29, 2022. [Online]. Available: https://bit.ly/3rb6srU
[48] T. Hussain, S. Suryanarayanan, and S. M. S. Alam, "Hybridized transmission switching for contingency management in electric power systems," International Application Patent PCT/US2 126 540, Apr. 9, 2021.

TANVEER HUSSAIN (Graduate Student Member, IEEE) received the B.E. degree in electrical engineering from the National University of Sciences and Technology, Islamabad, Pakistan, and the M.S. degree in electrical engineering from the Politecnico di Milano, Milan, Italy. He is currently pursuing the Ph.D. degree in electrical engineering with the Electrical Engineering and Computer Science Department, South Dakota State University. His research interests include the topic of wide-area transmission systems and minimization of load shedding.

SIDDHARTH SURYANARAYANAN (Senior Member, IEEE) was born in Chennai, India. He received the Ph.D. degree in electrical engineering from Arizona State University.

TIMOTHY M. HANSEN (Senior Member, IEEE) received the B.S. degree in computer engineering from the Milwaukee School of Engineering, Milwaukee, WI, USA, in 2011, and the Ph.D. degree in electrical engineering from Colorado State University, Fort Collins, CO, USA, in 2015.

He is currently an Associate Professor with the Electrical Engineering and Computer Science Department, South Dakota State University, Brookings, SD, USA. His research interests include the areas of optimization, high-performance computing, and electricity market applications to sustainable power and energy systems, low-inertia power systems, smart cities, and cyber-physical-social systems.

Dr. Hansen is an Active Member in ACM SIGHPC. He was a recipient of the 2019 IEEE-HKN C. Holmes MacDonald Outstanding Teaching Award. He was the inaugural recipient of the Milwaukee School of Engineering Graduate of the Last Decade Award, in 2020. Within IEEE, he has been the IEEE Siouxland Section Chair (since 2019). He is active within the IEEE PES Power Engineering Education Committee, serving as the Awards Subcommittee Chair and a Research Subcommittee Secretary-Elect.

S. M. SHAFIUL ALAM (Senior Member, IEEE) received the B.S. and M.S. degrees in electrical and electronic engineering from the Bangladesh University of Engineering and Technology, Dhaka, Bangladesh, in 2008 and 2011, respectively, and the Ph.D. degree in electrical engineering from Kansas State University, Manhattan, KS, USA, in 2015.

He is currently a Research Scientist with the Idaho National Laboratory, ID, USA, and works with the Power and Energy Systems Group, EES&T Directorate. His current research interests include the areas of reliable and sustainable integration of energy systems, specially the modeling and validation of the operation and control of hybrid energy systems through digital real-time simulation with hardware-in-the-loop testing.